Journal of Biomedical Optics

SPIEDigitalLibrary.org/jbo

Endoscopic optical coherence tomography device for forward imaging with broad field of view

Anke Burkhardt
Julia Walther
Peter Cimalla
Mirko Mehner
Edmund Koch

SPIE

Endoscopic optical coherence tomography device for forward imaging with broad field of view

Anke Burkhardt, Julia Walther, Peter Cimalla, Mirko Mehner, and Edmund Koch
Dresden University of Technology, Faculty of Medicine Carl Gustav Carus, Department of Clinical Sensoring and Monitoring, Fetscherstr. 74, 01307 Dresden, Germany

Abstract. One current challenge of studying human tympanic membranes (TM) with optical coherence tomography (OCT) is the implementation of optics that avoid direct contact with the inflamed tissue. At the moment, no commercial device is available. We report an optics design for contactless forward imaging endoscopic optical coherence tomography (EOCT) with a large working distance (WD) and a broad field of view (FOV) by restricting the overall diameter of the probe to be small (3.5 mm), ensuring a sufficient numerical aperture. Our system uses a gradient-index (GRIN) relay lens and a GRIN objective lens, and executes a fan-shaped optical scanning pattern. The WD and FOV can be adjusted by manually changing the distance between the triplet and the GRIN relay lens. The measured lateral resolution is ~28 μm at a WD of 10 mm with a FOV of 10 mm. Additionally, a camera and an illumination beam path were implemented within the probe for image guidance during investigations of the TM. We demonstrated the performance of the EOCT design by 3-D imaging of a human TM *ex vivo* and *in vivo* with a k-linear spectral domain OCT system. [DOI: 10.1117/1.JBO.17.7.071302]

Keywords: endoscopic optical coherence tomography; gradient index; field of view; tympanic membrane.

Paper 11561SS received Sep. 30, 2011; revised manuscript received Nov. 29, 2011; accepted for publication Dec. 5, 2011; published online May 16, 2012.

1 Introduction

Endoscopic optical coherence tomography (EOCT) is receiving increasing attention because this imaging technique has the potential to visualize subsurface structures inside cavities and hollow organs. EOCT devices can be classified as either forward or side imaging. In general, side imaging OCT probes are two-dimensional (2-D) in nature. These probes commonly consist of a fiber, a lens for focusing, and a prism for lateral deflection of the light. The combination of rotational side imaging and back-and-forth translation of the probe is used to generate three-dimensional (3-D) images.[1–3] Side imaging probes are used for imaging hollow organs, such as the intravascular system or the gastrointestinal tract.[3,4] In comparison, forward imaging probes are more technically challenging because the generation of a 3-D image cannot be realized by the back-and-forth translation. To achieve 3-D information of the investigated structures, scanning is realized by, e.g., a piezoelectric transducer, galvanometer scanners, or a microelectromechanical system.[5–7] That makes it very difficult to maintain the overall diameter small and still achieve a large working distance (WD) and a broad field of view (FOV). While being immune against normal vibrations, forward imaging probes are needed in different application areas, such as gynecology, urology, or otorhinolaryngology.[8–10] The intention of our research was to develop a suitable EOCT device especially for imaging the tympanic membrane (TM) and behind it. Because the TM lies at the end of the auditory canal, EOCT is intended to detect diseases of the TM and the middle ear, such as otitis media or cholesteatoma.[10–12] Cholesteatomas show characteristic findings in OCT imaging that differentiate them from healthy tissues.[10] The detection of otitis media by otoscopy is still difficult, even for a specialist. Chronic cases of otitis media are accompanied by a bacterial biofilm behind the TM that could be visible with OCT, but cannot be detected with a regular otoscope.[12] OCT allows depth-resolved imaging of the TM and structures behind it and creates new opportunities in disease detection.[13] It could be possible to distinguish between the acute and chronic form and thereby avoid the overuse of antibiotics that are not necessary in a chronic case and can lead to resistant bacteria.[12] Also swelling and inflammation of otitis media could be visible in earlier stages. To avoid direct contact to the inflamed tissues and allow imaging of the entire TM, an EOCT system with a large WD and a broad FOV is necessary. Because of the position of the TM, a forward imaging probe is more feasible. Furthermore, we decided to develop a rigid probe because the generation of a 3-D image can be executed outside the body. There are no moving parts inside the auditory canal that are required for 3-D imaging, allowing us to achieve a smaller probe diameter. Additionally, rigid optics designs still have a better optical quality in contrast to fiber-optic bundles,[14] so the axial and lateral resolution can be kept in a sufficient region to allow the visualization of microstructures of the investigated tissues.

2 Materials and Methods

2.1 *Endoscopic Optics*

The optics of the EOCT scanning unit consisted of a collimator for light coupling; two galvanometer scanners for 3-D imaging; a triplet (Edmund Optics, Barrington, New Jersey, NT45-251), a gradient-index (GRIN) relay lens (GRINTECH GmbH, Jena, Germany, GT-IFRL-200-100-10-NC), a GRIN objective lens

Address all correspondence to: Anke Burkhardt, Dresden University of Technology, Faculty of Medicine Carl Gustav Carus, Department of Clinical Sensoring and Monitoring, Fetscherstr. 74, 01307 Dresden, Germany. Tel: +49(0)351 458 6135; Fax: +49(0)351 458 6325; E-mail: anke.burkhardt@tu-dresden.de.

0091-3286/2012/$25.00

(GRINTECH GmbH, Jena, Germany, GT-IFRL-200-010-50-NC) for OCT imaging; and glass fibers for illumination (Fig. 1). Additionally, a dichroic mirror, which is reflective for infrared and transparent for visible light, allowed the coupling of the camera beam path into the sample arm for online video image guidance in the visible (VIS) spectral range [Fig. 2(b)]. In the camera beam path the light from the sample arm was focused by a lens on the CMOS video camera sensor. That opened the opportunity to match the focus for VIS imaging to the focus of the OCT beam path. The collimator and the triplet were chosen for using the whole numerical aperture (NA) of 0.1 of the GRIN relay lens. An enhancement of the NA is possible but would result in an undesired shortening of the GRIN relay lens length, and the combination of multiple relay lenses would lead to a worsening of the optical aberrations. The 1.0 pitch GRIN relay lens allows image guidance over a long distance and is about 100 mm in length and 2 mm in diameter. The lens was chosen for its sufficient length for imaging the TM inside the auditory canal (the length of which is approximately 30 mm), as well as its small diameter. A GRIN objective lens with an NA of 0.5 was placed into the sample arm for the realization of both a large WD and a broad FOV. Additional VIS illumination was achieved by the use of glass fibers. For this, an adapter was designed that arranged the glass fibers around the GRIN relay lens in a ring shape (Fig. 1). The glass fibers were supplied with VIS light by a high power SMD LED (surface-mounted device light emitting diode), which was installed on the housing of the scanner head. The GRIN optics and the glass fibers were housed in a metal tube for protection, which gave an overall diameter of 3.5 mm. To improve the OCT image quality, we corrected the optics for dispersion using glass compensation in the reference arm. Therefore, a similar GRIN relay lens was inserted. To avoid additional surfaces, this relay lens further acts as the reference mirror by carrying a gold layer on the end surface (Fig. 2). The achieved depth resolution after dispersion compensation was approximately 7.6 μm compared with 6.4 μm without the additional GRIN optics.

2.2 *System Setup*

The forward endoscopic optical coherence tomography (EOCT) probe with integrated Michelson interferometer is fiber coupled with a self-designed standalone k-linear spectrometer. The setup of the spectrometer is displayed in Fig. 2. The short coherent

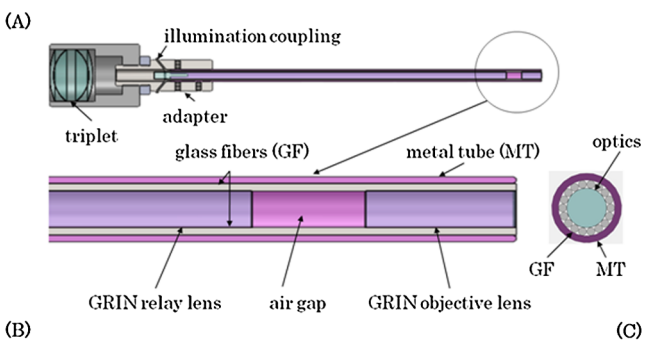

Fig. 1 Schematic of the endoscopic configuration. (a) A triplet is used to focus the incident light inside the GRIN relay lens. This lens guides the light to its distal end and focuses it on the surface of the GRIN objective lens and the GRIN objective lens focuses the beam on the sample. (b) The whole optics and the illumination are housed in a metal tube. (c) Top view of the distal end of the EOCT device.

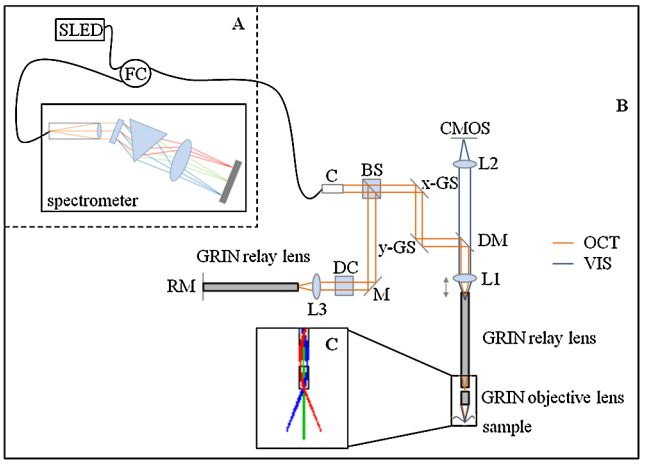

Fig. 2 Endoscopic optical coherence tomography (EOCT) spectral domain setup. (a) Superluminescent light-emitting diode (SLED), standalone spectrometer, and fiber coupler (FC). (b) Optics of the scanning unit of the EOCT device with integrated Michelson interferometer. The light from the collimator (C) is split by the beam splitter (BS) into reference and sample arm. GS: galvanometer scanner, DM: dichroic mirror, CMOS: video camera sensor, M: mirror, DC: dispersion compensation, RM: reference mirror, L1: triplet, L2, L3: lenses, GRIN: gradient index lens. Orange: OCT beam path, blue: VIS beam path. (c) Fan-shaped optical scanning pattern.

light source used is a superluminescent light-emitting diode (SLED EXS8810-2411, Exalos AG) with a center wavelength of 880 nm, a full width half maximum of 65 nm, and an optical power of 4 mW. For the infrared beam path, the light from the collimator is split by a beam splitter into reference arm and sample arm (Fig. 2). Three-dimensional OCT imaging is realized by deflecting the light by two orthogonal aligned galvanometer scanners. The light is focused by the triplet and scanned laterally over the GRIN relay lens. The focus of the triplet was shifted behind the proximal surface of the GRIN relay lens, inside the lens. The GRIN relay lens then guides the light from one side to the other, so that the focus shift from the proximal end is transferred to the distal end. This shift avoids disturbing reflexes from the plane surfaces of the GRIN relay lens and has no further negative influence on imaging. The GRIN objective lens was then inserted 4 mm behind the GRIN relay lens. The NA of 0.5 allowed a fan-shaped optical scanning pattern that was important to achieve a broad FOV [Fig. 2(c)]. By adjusting the distance between the triplet and the GRIN optics, a change in WD can be realized. The backscattered light from within the sample and the reference light are superimposed and directed to the k-linear spectrometer, consisting of a transmission grating, dispersion prism and a line detector. The detector operated at a readout rate of 11.90 kHz. The system had a sensitivity of 102 dB and achieved a depth range of approximately 3 mm.

3 Experimental Results

3.1 *Specifications of the Optics*

EOCT is required to detect diseases of the TM and the middle ear. To avoid direct contact with the inflamed tissues and allow imaging of the entire TM, EOCT systems must have a large WD and a broad FOV. Thus, we designed gradient index optics for forward EOCT imaging. Our scanner head had a maximum WD of ~10 mm with a corresponding FOV of ~10 mm [Fig. 3(c)

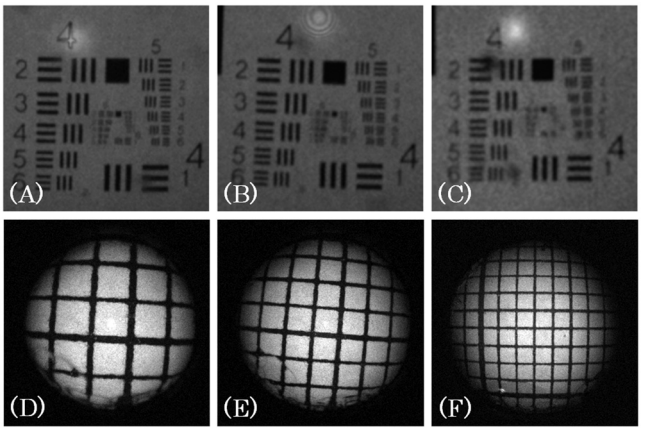

Fig. 3 Images taken for measuring the lateral resolution (Δx) and field of view (FOV) in dependence of the adjusted working distance (WD). (a)–(f) The three-dimensional OCT-data cube was averaged in axial direction. As the information is concentrated in a few planes this is similar to an *enface* image of the deformed plane. (a)–(c) USAF resolution test target. (d)–(f) millimeter paper. (a) Δx ~20 μm in a WD of ~5 mm with corresponding FOV of ~5 mm (d). (b) Δx ~22 μm in a WD of ~7 mm with a FOV of ~7 mm (e) and (c) Δx of ~28 μm in a WD of ~10 mm with a FOV of ~10 mm (f). Unfortunately, some fissures of the distal end of the gradient index (GRIN) relay lens are visible in the boundary area of the FOVs.

and 3(f)], thus allowing the entire TM, which is generally 10 mm in diameter, to be imaged in one view. The lateral resolution was dependent on the WD; the shorter the WD, the better the lateral resolution. We measured the lateral resolution by OCT with the United States Air Force (USAF) resolution test target, finding that a WD of ~10 mm resulted in a lateral resolution of ~28 μm, WD of ~7 mm in a lateral resolution of ~22 μm, and WD of ~5 mm in a lateral resolution of ~20 μm [Fig. 3(a)–3(c)]. Similarly, we found that the FOV was dependent on the WD. We determined the FOV by OCT with a millimeter paper test chart, detecting a FOV of ~10 mm at a WD of ~10 mm, ~7 mm at a WD of ~7 mm, and ~5 mm at a WD of ~5 mm [Fig. 3(d)–3(f)]. The data correspond to our calculated theoretical lateral resolutions: ~25 μm at 10 mm, ~21 μm at 7 mm, and ~18 μm at 5 mm (Fig. 4). The theoretical data were determined with the lens equation, treating the GRIN lenses as ideal lenses. If a better lateral resolution than 28 μm is necessary, an enhancement is possible by adjusting the distance between the triplet and the GRIN relay lens in the sample arm. This change in distance resulted in a shortening of the WD. Furthermore, a smaller FOV that could be beneficial for smaller TMs, such as the TMs of children, could be achieved through the distance change.

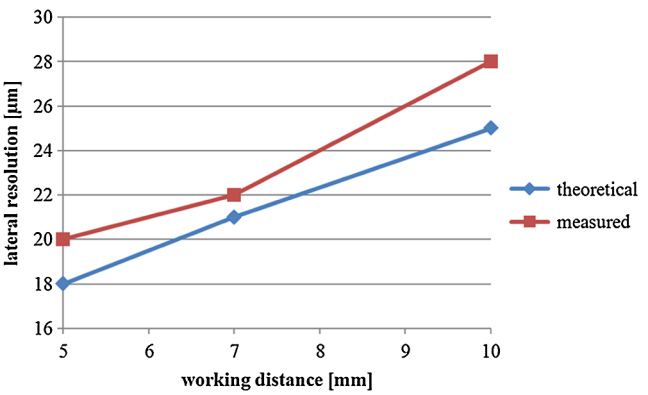

Fig. 4 Measured and theoretical lateral resolution of the OCT beam path in different working distances. The measured resolution (red line) was determined with the USAF resolution test target. The theoretical curve (blue line) was determined from the lense equation.

3.2 *Image Correction*

In the case of our endoscopic optics, the use of the fan-shaped optical scan pattern caused a field curvature. The position of the beam intersection is dependent of the image height, so that an object point that was far away from the optical axis resulted in an image point, which was shifted in axial direction. That means that the image was not generated on a plane, but on a curved surface. In the favorable case of imaging, the TM the cone form of the TM is faced in the same direction, much like the field of curvature caused by the fan-shaped scanning optics, achieving good image quality for that special case. Nevertheless, a slight error remained and the images had to be corrected (Fig. 5). At first, they were rescaled to achieve equal resolutions in X- and Y-direction and afterwards they were transferred to a linear scan by means of a digital unwrap image process. In this process, a selected region was unwrapped from a circular strip, like the surface of the millimeter paper in Fig. 5(a), to a rectangular strip [Fig. 5(b)] by the use of a coordinate transformation and a linear interpolation in both X- and Y-direction to compute the pixel location. First of all, we tested the correction on a millimeter paper and then on a human TM [illumination and camera beam 5(c) and 5(e)].

3.3 *TM Imaging Ex vivo*

We tested the performance of our EOCT device by 3-D imaging a human TM *ex vivo*. Representative OCT images are shown in Fig. 6. Typical regions of the TM, such as the manubrium of malleus (MM), were detected and a 3-D OCT image of the whole TM was recorded. A cross-section of the TM in the region of the umbo, the deepest point in the cone of the TM and a part of the MM were visible [Fig. 6(a) and 6(b)]. We also tested the

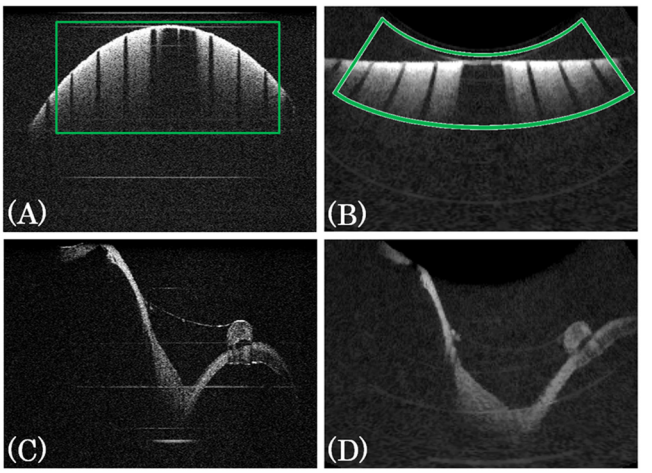

Fig. 5 Image correction. Optical coherence tomography (OCT) cross-sectional image of a millimeter paper (a) and the coressponding corrected image (b) and an OCT cross-sectional image of a TM (c) with the corrected image (d). The green boxes show the coordinate transformation.

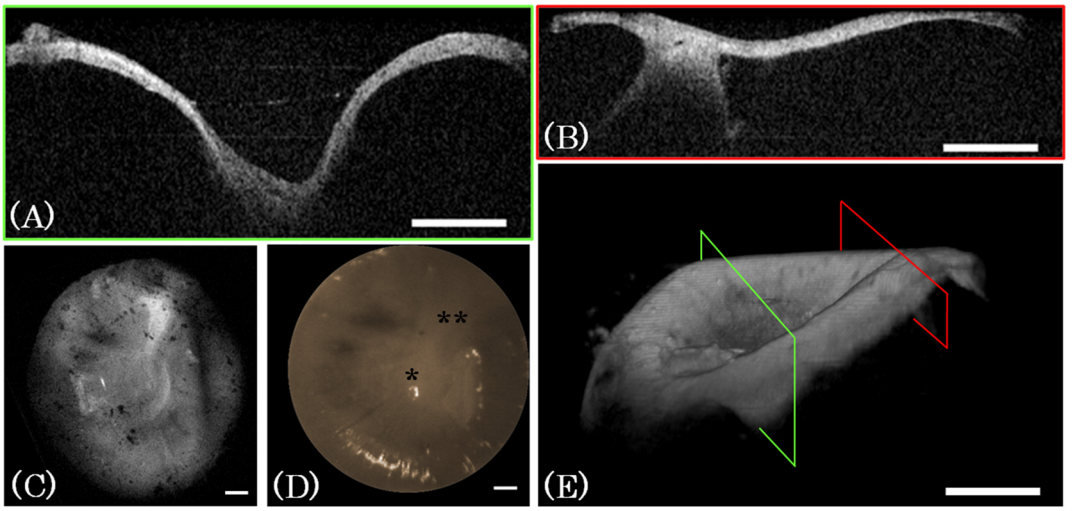

Fig. 6 Representative images of a tympanic membrane (TM) *ex vivo* acquired with the endoscopic setup. Optical coherence tomography (OCT) cross-sectional images through (a) the umbo, the deepest point of the TM, and (b) a part of the manubrium of malleus (MM). (c) top view OCT image of the TM and (d) top view camera picture of the TM acquired with the integrated VIS illumination, the umbo (*) and the MM (**) can be identified. (e) 3-D OCT image of the TM. Red and green frame belong to the position of (a) and (b). Scale bars correspond to a distance of 1 mm (Video 1, MPEG, 1.23 MB) [URL: http://dx.doi.org/10.1117/1.JBO.17.7.071302.1]

additional illumination and camera beam path [Fig. 6(d)], finding that our system is suitable to image the whole TM inside the auditory canal with one view. Different regions of the TM such as the umbo or the MM could be distinguished in the VIS 2-D enface image, thus providing additional video image guidance during the investigation. The cone form of the TM was clearly visible when acquiring OCT images of the whole TM [Fig. 6(e)].

3.4 *TM Imaging In vivo*

In a recent study, we tested the performance of our EOCT device by imaging a human TM *in vivo*. Therefore, a healthy human volunteer was positioned on a headrest and the examiner inserted the distal end of the endoscopic setup into the auditory canal. A camera image with the executed scan pattern is visible [Fig. 7(a)]. The corresponding B-scans in *X*- and *Y*-direction showed the suitability to distinguish between different regions of the TM. In the X-scan, a part of the MM was discernible, and in the Y-scan, some other ossicular structures and some bony structures behind the TM could be detected [Fig. 7(b) and 7(c)]. Additional a VIS 2-D enface image was acquired showing the feasibility of the camera beam path in the *in vivo* situation [Fig. 7(d)]. Thus, our EOCT device is suitable for imaging the TM *in vivo*.

4 Discussion

We developed a suitable EOCT device because there is a clinical need for the detection of diseases concerning the TM and the middle ear. The system should achieve a large WD to avoid direct contact to the inflamed tissues and a broad FOV to allow acquiring images of the whole TM with one recording. For this, we designed a gradient index optics for forward EOCT imaging. In comparison to the previous work reported so far, this is the first forward imaging endoscopic system achieving a broad FOV while maintaining the overall diameter of the probe small, achieving a ratio of approximately 1:3 (overall diameter:FOV). The smallest reported forward imaging probe has an outer diameter of 0.82 mm and was developed for ophthalmic OCT.[15] The optical setup consists of two counteracting gradient index (GRIN) lenses. This probe achieves a WD of approximately 0.78 mm and has a maximum tilt angle of 15.3-deg, not sufficient for the aforementioned application. The EOCT probe with the broadest FOV that has been presented thus far achieves a FOV of 6 mm, but has a large oval diameter of 7.5×3 mm.[7] This system was developed for arthroscopic OCT. The optical layout mainly consists of a scan lens. The forward imaging probe with the largest WD reported so far achieves an adjustable WD up to 7.5 mm, and was developed for example for thoracoscopic imaging of pleural cancer.[16,17] Unfortunately, the FOV is

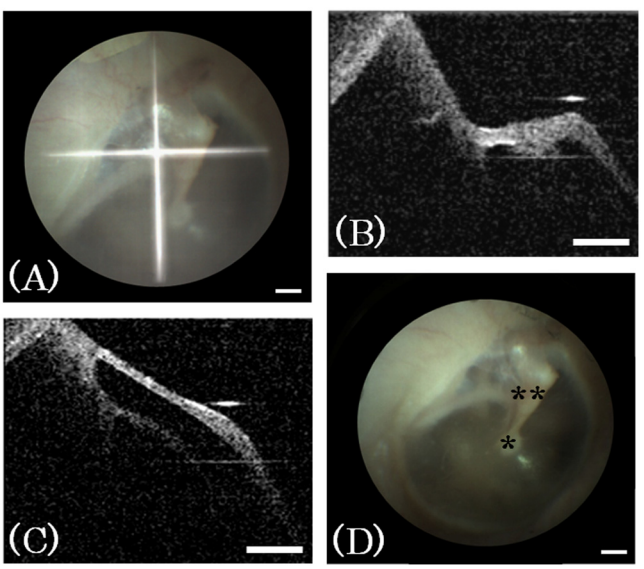

Fig. 7 Representative images of a tympanic membrane (TM) *in vivo* acquired with the endoscopic setup. (a) 2-D VIS camera image showing the scan pattern. OCT cross-sectional images through (b) a part of the manubrium of malleus in X-scan direction and (c) a part of rest of the ossicular chain and some bony structures in Y-scan direction. (d) Top view camera picture of the TM acquired with the integrated VIS illumination, the umbo (*) and the MM (**) can be identified. Scale bars correspond to a distance of 1 mm.

limited by the diameter of the selected lens and is 4.5 mm by a nearly similar overall diameter of the probe. In this optical setup, a GRIN relay lens was chosen. A further system mentioned in the literature for side imaging with large WD could easily be adapted to forward imaging by taking away the prism, but show other drawbacks solved with our design. The works of Yu et al.[18] and Guo et al.[19] describe this system that operates at a WD of 65 mm with a lateral scanning range of 5 mm. The setup is realized in a "double-barreled" configuration with the video endoscope separated from the OCT device. That leads to an unnecessary enlargement of the overall diameter. In general, the WD can be increased arbitrarily but result in a worsening of the numerical aperture and thus of the amount of light back scattered from a target. A compromise has to be found to achieve a feasible WD and FOV, and anyhow a sufficient numerical aperture and overall diameter of the probe. In our EOCT device, the camera beam path follows the same way as the OCT beam path. That allows keeping the diameter of the probe much smaller and because of the suitable NA for OCT a sufficient image quality was achieved.

5 Conclusion

In summary, we developed a new design for 3-D forward imaging endoscopic OCT. The system allows images to be acquired at a large WD with a large FOV. This is done by maintaining the outer diameter for the distal end small, and consequently enables access to cavities not accessible with bulky optics. When applying this to imaging the TM, a rigid GRIN optics design allows the development of a probe with an outer diameter not larger than 3.5 mm to gain access through the auditory canal. In addition, a camera beam path and illumination via glass fibers were incorporated into the probe, enabling video endoscopy inside cavities. *Ex vivo* and *in vivo* investigations with the EOCT device were performed. Thus, the developed device is suitable for acquiring images of the TM. An application in other medical or industrial fields is also feasible.

Acknowledgments

This research was supported by funding from the European Union (ESF) and the Free State of Saxony (project 080937940) and the SAB (Sächsische Aufbaubank, project 14302/2475).

References

1. Z. Yaqoob et al., "Methods and application areas of endoscopic optical coherence tomography," *J. Biomed. Opt.* **11**(6), 063001 (2006).
2. W. Kang et al., "Endoscopically guided spectral-domain OCT with double-balloon catheters," *Opt. Express* **18**(16), 17364–17372 (2010).
3. H. G. Bezerra et al., "Intracoronary optical coherence tomography: a comprehensive review," *J. Am. Coll. Cardiol.* **2**(11), 1035–1046 (2009).
4. W. Hatta et al., "Optical coherence tomography for staging of tumor infiltration in superficial esophageal squamous cell carcinoma," *Gastrointest. Endosc.* **71**(6), 899–906 (2010).
5. S. Moon et al., "Semi-resonant operation of a fiber-cantilever piezotube scanner for stable optical coherence tomography," *Opt. Express* **18**(20), 21183–21197 (2010).
6. J. Sun and H. Xie, "MEMS-based endoscopic optical coherence tomography", *Int. J. Opt.* **2011**, 1–12 (2011), .
7. Y. Pan et al., "Hand-held arthroscopic optical coherence tomography for in vivo high-resolution imaging," *J. Biomed. Opt.* **8**(4), 648–654 (2003).
8. J. K. S. Gallwas et al., "Optical coherence tomography for the diagnosis of cervical intraepithelial neoplasia," *Lasers Surg. Med.* **43**(3), 206–212 (2011).
9. E. Zagayanova et al., "Endoscopic OCT with forward-looking probe: clinical studies in urology and gastroenterology," *J. Biophoton.* **1**(2), 114–128 (2008), .
10. H. R. Djalilian et al., "Optical coherence tomography of cochlesteatoma," *Otol. Neurotol.* **31**(6), 932–935 (2010).
11. H. R. Djalilian et al., "Imaging the human tympanic membrane using optical coherence tomography in vivo," *Otol. Neurotol.* **29**(8), 1091–1094 (2008).
12. C. T. Nguyen et al., "Non-invasive optical interferometry for the assessment of biofilm growth in the middle ear," *Biomed. Opt. Express* **1**(4), 1104–1116 (2010).
13. A. Burkhardt et al., "Endoscopic optical coherence tomography for imaging the tympanic membrane," *Proc. SPIE* **8091**, 80910Y (2011).
14. W. Wang et al., "Comparison of different focusing systems for common-path optical coherence tomography with fiber-optic bundle as endoscopic probe," *Opt. Eng.* **48**(10), 103001–1030018 (2009).
15. S. Han et al., "Handheld forward-imaging needle endoscope for ophthalmic optical coherence tomography," *J. Biomed. Opt. Lett.* **13**(2), 020505 (2008).
16. T. Xie, S. Guo, and Z. Chen, "GRIN lens rod based probe for endoscopic spectral domain optical coherence tomography with fast dynamic focus tracking," *Opt. Express* **14**(8), 3238–3246 (2006).
17. T. Xie et al., "In vivo three-dimensional imaging of normal tissue and tumors in the rabbit pleural cavity using endoscopic swept source optical coherence tomography with thoracoscopic guidance," *J. Biomed. Opt.* **14**(6), 064045 (2009).
18. L. Yu et al., "Office-based dynamic imaging of vocal cords in awake patients with swept-source optical coherence tomography," *J. Biomed. Opt.* **14**(6), 064020 (2009).
19. S. Guo et al., "Gradient-index lems rod based probe for office-based optical coherence tomography of the human larynx," *J. Biomed. Opt.* **14**(1), 014017 (2009).